

Responses to Reviewers' Comments

Journal: Atmospheric Chemistry and Physics

Manuscript ID: ACP 2015-926

Manuscript Title: Bi-directional air-sea exchange and accumulation of POPs (PAHs, PCBs, OCPs and PBDEs) in the nocturnal marine boundary layer

Authors: Gerhard Lammel, Franz X. Meixner, Branislav Vrana, Christos Efstathiou, Jiří Kohoutek, Petr Kukučka, Marie D. Mulder, Petra Příbylová, Roman Prokeš, Tatsiana P. Rusina, Guo-Zheng Song, Manolis Tsapakis

We would like to thank the reviewers for their thoughtful reading, comments and questions, which considerably helped to improve this manuscript. We have addressed all comments below and have indicated the corresponding modifications in the revised version of the manuscript. All the changes are tracked in the manuscript. The line numbers mentioned in our responses to the comments refer to those in the submitted manuscript (please see attached).

Anonymous Referee #2

Received and published: 24 March 2016

This study presents bi-directional fluxes of a number of POPs generated from gradient measurements made at a remote coastal site. Such data are needed for improving our understanding of the sources and fates of POPs over ocean surfaces, although the measurements could cover longer periods and for more POPs species with high-volume sampling. A box chemistry model is also used to explain the observed data and to improving the understanding of the air-surface exchange processes. The paper is generally well written and only some minor comments are provided below.

Line 211 and lines 182-185: Briefly explain if the insignificant gradients were caused by uncertainties in the measurement, or they represent the situation that fluxes were minimal.

Small fluxes cannot be distinguished from measurement uncertainties. The criterion to identify gradients is given in the text.

Line 391 and line 399: two contradictory statements. “0.0043 cm/s, significantly deviating from zero”, and “0.020 cm/s, not distinguishable from zero”.

Refers to the ranges spanned by a number of flux measurements specified in the text. These were $0.0043 \pm 0.0031 \text{ cm s}^{-1}$ and $0.020 \pm 0.032 \text{ cm s}^{-1}$, respectively. The criterion to identify distinguishability is now identified in the text. The new text reads: “ $0.0043 \pm 0.0031 \text{ cm s}^{-1}$, still significantly deviating from zero (1 standard deviation criterion).” and “not distinguishable from zero e.g., $0.020 \pm 0.032 \text{ cm s}^{-1}$ for α -HCH and $0.011 \pm 0.015 \text{ cm s}^{-1}$ for PCB28 (1 standard deviation criterion).”

Lines 427-428: “wet deposition not significant” - because of small amount of precipitation, or particle size range?

Small amount of precipitation. Now specified.

Lines 439-440: delete the statement. Vd is sensitive to friction velocity (and wind speed) over any surface (see Zhang and He, 2014, ACP 14, 3729-3737).

Will be done

Line 449-450: should not compare a single size since any particle species covers a size range (i.e., a size distribution). A representative size does not mean it has a representative deposition velocity (see Ruijgrok et al., 1997, Tellus 47B 587-601).

Yes, thank you for pointing this out. As the difference between gaseous and particulate deposition fluxes (at the site during the measurements) was ≈ 3 orders of magnitude, the estimate made still leads to the same qualitative statement. This discussion will be correspondingly extended in the revised version. New text will read: “Furthermore, values of v_{dep} integrated over the entire size spectrum may differ considerably from values of v_{dep} for MMD (Ruijgrok et al., 1995). However, even then, particle deposition is unlikely to have significantly compensated for net-volatilization, as even for particles grown to $1.5 \mu\text{m}$ $F_{\text{p dep}}$ would be higher by not more than a factor of 10 (Slinn and Slinn, 1980).”

Ruijgrok, W., Davidson, C.I., and Nicholson, K.W.: Dry deposition of particles – implications and recommendations for mapping of deposition over Europe. *Tellus B*, 47, 587-601, 1995.

Same case for Line 463. Also 0.3 cm/s seems to be on the high end for submicron particles.

Yes, should account for more uncertainty. However and again, as the difference between gaseous and particulate deposition fluxes was ≈ 2 orders of magnitude in this case, the estimate made still leads to the same qualitative statement. The correspondingly modified text will read: “Hereby, $v_{\text{dep}} = 0.05\text{-}0.3 \text{ cm s}^{-1}$ was adopted to account for mass median diameters ranging $0.5\text{-}1.5 \mu\text{m}$...”

Proofread the paper for fixing the editorial issues, e.g., Line 71 “to to”; line 73 “the highest”; line 458 “of for”.

Will be done

Anonymous Referee #3

This paper described a study of the gas and particle deposition flux of POPs over the marine boundary layer based on vertical gradient measurements. The results indicate both upward and downward fluxes of POPs occurred, and the direction of the fluxes changed frequently for some POPs. Emissions of POPs were driven by volatilization from the sea during daytime and nighttime for some POPs. Long-term measurements are needed to validate the results and apply them to modeling studies. This paper is suitable for publication after addressing the comments below.

Line 34: This sentence is not necessarily specific to the marine atmospheric environment; continental atmospheres are also impacted by land sources and contaminated soil emissions of POPs.

True, but will be left unchanged, as the statement itself is correct and nothing is or is intended to be said about continental atmospheres.

Please also correct the grammar error, “which are advected from sources on land, primary and secondary, such as volatilization from contaminated soils”. I suggest revising to, “which are advected from primary sources on land and secondary sources, such as volatilization from contaminated soils.”

To be corrected by shortening. The new text will read: “The marine atmospheric environment is a receptor for persistent organic pollutants (POPs) which are advected from primary and secondary sources on land.”

Lines 42-43: What are the sources of POPs to surface waters that can lead to a buildup of concentrations? Does deposition alone lead to elevated POP concentrations in surface water?

Will be specified. The new text will read: “...fed by riverine or atmospheric deposition input.”

Lines 80-81: Please explain why these two heights were chosen for determining the vertical gradient. How does height selection potentially affect the vertical concentration and flux gradients?

Will be explained. The new text will read: "According to the Monin-Obukhov similarity theory of turbulent transport in the surface layer (Monin and Obukhov, 1954; s. supplement, sect. S1.3), vertical concentration profiles are expected to be logarithmic, while – due to the vertically non-linear behaviour of the eddy diffusivity – the resulting vertical flux is *per definitionem* constant. For a given surface source (sink) of gases or particles corresponding negative (positive) vertical concentration gradients ($\partial c/\partial z$) will be maximal close to the source (sink). Therefore, over aerodynamically smooth surfaces, the lower inlet height should be preferably in the order of a few tenths of a meter, while the distance to the upper inlet height, should be maximized to yield large (and consequently statistically significant) vertical concentration differences. However, the choice for the upper inlet height is limited by the horizontal extension of the so-called "fetch", i.e. the up-wind surface homogeneity (in terms of orography, structure, and vegetation), which should be at least $100 \times z_2$ (e.g. Foken, 2008). In the case of our study, the choice of the lower inlet height ($z_1=1.05$ m) is just due to the design of the aerosol sampler which does not allow sampling below 1.05 m above ground, while the upper inlet height ($z_2=2.80$ m) accounts for the limited surface homogeneity (200 m) of the Selles Beach site."

Line 146: All equations should be labeled with numbers as well as in the text chronologically.
Will be done

Line 223: I suggest replacing with "universal gas constant R (Pa m³ mol⁻¹ K⁻¹), and both sea surface temperature (SST or T_w) and salinity corrected: : :"
Will be done

Lines 277-283: Only gas-phase pollutants are volatilize from the sea surface. Please mention if the ratios are based on gas-phase concentrations or gas+particulate concentrations and include the range of these ratios over the sampling period in addition to the average.

Will be specified. The new text will read: "For PAHs the mean ratio of day/night concentrations (gaseous only), $c_{\text{day}}/c_{\text{night}}$, was 0.67 (0.54-0.85) for ACE, while $c_{\text{day}}/c_{\text{night}}$ ranged wider, 0.25-3.35, for PHE, FLT and PYR, with mean values of $c_{\text{day}}/c_{\text{night}} = 1.41-1.53$."

Lines 283-284: What could be the reasons for the lower $C_{\text{day}}/C_{\text{night}}$ ratio for chlorinated compounds specifically?

Thanks for pointing this out. The individual data indicate that there is no significant trend hidden. More in depth analysis for a sub-set of samples is presented later in the text (section 3.5). The new text will read: "For chlorinated substances, we find mean $c_{\text{day}}/c_{\text{night}} < 1$, namely 0.56-0.66 for HCH isomers, and 0.68-0.94 for PCBs and DDE, while the individual values range widely, 0.04-4.8."

Lines 302-304 and lines 329-336: Volatilization tends to occur during daytime. Please explain how this process contributes to the elevated nighttime concentrations. Could wind speed be another factor controlling volatilization of gases other than temperature?

Volatilization tends to occur during daytime driven by surface heating during the day and surface cooling during the night – which was not the case during the measurements reported here ($SST_{\text{day}} - SST_{\text{night}} = 0.1-0.9$ K, see Table S4). Other processes overcompensated for this small difference in SST, the most prominent being variation of mixing depth (low during the night, high during the day). This hypothesis is tested with the non-steady state 2-box model (presented in section 2.6).

Lines 336-341: The temperature difference between daytime and nighttime (0.5-1.5K) is too small to explain the differences in daytime and nighttime concentrations and fluxes. What would be the corresponding difference on sea surface temperatures?

$SST_{\text{day}} - SST_{\text{night}} = 0.1-0.9 \text{ K}$ (see Table S4 and previous reply, above)

Lines 363-365: What are the implications of frequent changes in the direction of air-sea exchange in terms of estimating the deposition budget of POPs? If the fluctuations are so frequent, it would be difficult to obtain an accurate deposition budget.

True. The statement “Implicitly, dry deposition is difficult to budget.” will be added to the revised text. The same is/was expressed in the text (section 4, conclusions): “Both flux directions were observed (fluctuation) (...), not determined by the day-night cycle. Fluctuation of more substances might have been hidden by the method’s uncertainties. Hence, the mean flux direction on one hand side and observations during part of the time of the trace substances may differ. (...) In general, longer observations and across seasons of the flux is needed to assess the state of air-sea exchange of those anthropogenic trace substances, which have been approaching phase equilibrium historically (...) or seasonally (...)”

This text will be slightly extended in the revised text. “... In general, longer observations and across seasons of the flux is needed to assess dry deposition fluxes and the state of air-sea exchange ...”

Fig. 2: Label which series is the predicted and observed data.

Will be done

Lines 382-384: The vertical flux gradient of gases is based on a height difference of 1.8 m. How representative is this flux estimate of the overall deposition flux?

According to the Monin-Obukhov similarity theory of turbulent transport in the surface layer (Monin and Obukhov, 1954; see section S1.3), vertical concentration profiles are expected to be logarithmic, while – due to the vertically non-linear behaviour of the eddy diffusivity – the resulting vertical flux is *per definitionem* constant. New text to be added (in section 2.2, after line 1149): “As long as the vertical concentration gradient is statistically significant, and the choice of the upper inlet height accounts for the homogeneity of the up-wind so-called fetch (see above), the resulting flux, calculated from the transfer velocity and the vertical concentration gradient (see eq. (1)), is the vertical turbulent net flux of the corresponding gas, representative for the fetch area and equal to the overall deposition flux (if $c(z_2) - c(z_1) > 0$).”

Line 388: It is not clear which height the concentration corresponds to in this equation for determining the deposition velocity. Is it the average concentration of the two heights or just the ground-level concentration?

Thanks. Will be clarified in the revised text: “based on measurement at $z_1 = 1.05 \text{ m}$ ”

Line 422: New sentence is needed after “reason”

Will be done

Line 432: It is not clear which height the concentration corresponds to in this equation for determining the particle deposition flux.

Will be specified. Modified text will read: “ $F_{\text{p dep}} = -v_{\text{dep}} c_{\text{p}}$ (equ. 4) with v_{dep} being determined by particle size and wind speed and c_{p} determined close to the sea surface.”

Lines 446-450: The lack of particle size distribution data is a major source of uncertainty in the dry deposition flux calculations, since lower molecular weight PAHs are likely to partition

onto particles of various sizes. See the variation of aerosol dry deposition velocities with particle sizes in Petroff and Zhang (2010, Geoscientific Model Development).

We agree; 3-4 ring PAHs are expected to re-distribute in the aerosol mass size distribution. However, as the difference between gaseous and particulate deposition fluxes was anyway huge (≈ 3 orders of magnitude), the estimate made still leads to the same qualitative statement. This discussion will be correspondingly extended in the revised version. (see above, reply to Reviewer #2)

Lines 470-473: Could the upward flux of particulate-phase POPs be related to sea-salt emissions from waves?

Thanks for pointing this out. The particle source sea spray will contain POPs, whenever these were accumulated in surface waters. Therefore, upward flux could be related to waves (sea spray). Explanation will be given in the new text: “Marine aerosol contains organic matter (OM), mostly in the accumulation mode, in particular over biological productive surface waters and under low wind speeds (Gantt et al., 2011; Albert et al., 2012). A considerable part of OM is water insoluble (O’Dowd et al., 2004; Facchini et al., 2008). Hence, the marine aerosol contains traces of POPs, which previously were in either dissolved form or associated with suspended OM. The upward flux of particulate-phase POPs could be caused by sea spray.”

Albert, M.F.M.A., Schaap, M., Manders, A.M.M., Scannell, C., O’Dowd, C.D., and de Leeuw, G.: Uncertainties in the determination of global sub-micron marine organic matter emissions. *Atmos. Environ.*, 57, 289-300, 2012.
Facchini, M.C., Rinaldi, M., Decesari, S., Carbone, C., Finessi, E., Mircea, M., Fuzzi, S., Ceburnis, D., Flanagan, R., Nilsson, E.D., de Leeuw, G., Martino, M., Woeltjen, J., and O’Dowd, C. D.: Primary submicron marine aerosol dominated by insoluble organic colloids and aggregates, *Geophys. Res. Lett.*, 35, L17814, 2008.
Gantt, B., Meskhidze, N., Facchini, M.C., Rinaldi, M., Ceburnis, D., and O’Dowd, C.D., 2011. Wind speed dependent size-resolved parameterization for the organic mass fraction of sea spray aerosol. *Atmospheric Chemistry and Physics*, 11, 8777-8790, 2011.
O’Dowd, C.D., Facchini, M.C., Cavalli, F., Ceburnis, D., Mircea, M., Decesari, S., Fuzzi, S., Yoon, Y.J., and Putaud, J.P.: Biogenically driven organic contribution to marine aerosol. *Nature*, 431, 676-680, 2004.

Lines 492-493: The meaning of the sentence, “Fluctuation of more substances might have been hidden by the method’s uncertainties.” is unclear. Did you mean insufficient number of POPs analyzed or not enough samples collected?

Will be clarified in the new text by indicating for both PAHs and chlorinated species (Fig. 1a and 1b) and by rephrasing: “Fluctuation of more substances addressed might have been hidden by gaps in the time series of fluxes (limited by the uncertainties of sampling and analysis) or the time resolution (limited by the sensitivity of the analytical method).”

Title: The paper is lacking some discussion specifically on the accumulation of POPs in the nocturnal marine boundary layer, as stated in the title. I feel the paper discussed the diel variation (both daytime and nighttime) of POPs.

Findings of night-time maxima and accumulation were presented and discussed (sections 3.1 and 3.2, Fig. 1 and 2), also covered in the conclusions and abstract. But, yes, we agree, should be more emphasized. The revised text will read (in section 3.1, lines 288-289) “This results in night-time accumulation. Diel variation, apart from mixing, is related to ...” and (in section 3.2, lines 299-302) “The modelling results support that (during advection of one air mass) the diel variation of contaminant concentrations in air and, particularly, the night-time accumulation was explained by the combination of volatilisation from the sea surface and atmospheric mixing depth.” The visualized volatilization fluxes (Fig. S4) had not been referenced in the text. In the revised text this (lines 302-305) will read: “Volatilisation from the sea surface has significantly contributed to the night-time maxima of HCB (upward flux, Fig. 2a) and PCB28 (Fig. 2b), as well as of PYR during 1 night (Fig. S4a; Table S5). This, to

our knowledge, had never been observed before.” To this end, the corresponding flux plots (Fig. S4) will be moved to the main text (revised Fig. 2) and complemented by HCB (not shown in Fig. S4, but in revised Fig. 2). In the conclusions all substances for which observations (mentioned in lines 329-331) or modelling (lines 302-305) suggests that volatilization from the sea surface sustained night-time accumulation in the BL i.e., HCB, HCH, PCB28, PCB52 and PYR, will be mentioned (not just 1 of these as now, in line 481).

Supplement: There are two Table S6 in the supplement.

Thanks, will be corrected (Tables S6, S7).

1 **Bi-directional air-sea exchange and accumulation of POPs (PAHs, PCBs, OCPs and**
2 **PBDEs) in the nocturnal marine boundary layer**

3
4 Gerhard Lammel^{1,2*}, Franz X. Meixner³, Branislav Vrana¹, Christos Efstathiou¹, Jiří
5 Kohoutek¹, Petr Kukučka¹, Marie D. Mulder¹, Petra Příbylová¹, Roman Prokeš¹, Tatsiana P.
6 Rusina¹, Guo-Zheng Song³, Manolis Tsapakis⁴

7
8 ¹Masaryk University, Research Centre for Toxic Compounds in the Environment, Brno,
9 Czech Republic

10 ²Max Planck Institute for Chemistry, Multiphase Chemistry Dept., Mainz, Germany

11 ³Max Planck Institute for Chemistry, Biogeochemistry Dept., Mainz, Germany

12 ⁴Hellenic Centre for Marine Research, Institute of Oceanography, Gournes, Greece

13 * lammel@recetox.muni.cz

14
15 **Abstract**

16 As a consequence of long-range transported pollution air-sea exchange can become a major
17 source of persistent organic pollutants in remote marine environments. The vertical gradients
18 in air of 14 species i.e., 4 parent polycyclic aromatic hydrocarbons (PAHs), 3 polychlorinated
19 biphenyls (PCBs), 3 organochlorine pesticides (OCPs) and 2 polybrominated diphenylethers
20 (PBDEs) in the gas-phase were quantified at a remote coastal site in the southern Aegean Sea
21 in summer. Most vertical gradients were positive ($\Delta c/\Delta z > 0$) indicating downward (net
22 depositional) flux. Significant upward (net volatilisation) fluxes were found for 3 PAHs,
23 mostly during day-time, and for 2 OCPs, mostly during night-time, as well as for 1 PCB and 1
24 PBDE during part of the measurements. While phenanthrene was deposited, fluoranthene
25 (FLT) and pyrene (PYR) seem to undergo flux oscillation, hereby not following a day/night
26 cycle. Box modelling confirms that volatilisation from the sea surface has significantly

27 contributed to the night-time maxima of OCPs. Fluxes were quantified based on Eddy
28 covariance. Deposition fluxes ranged $-28.5 - +1.8 \mu\text{g m}^{-2} \text{d}^{-1}$ for PAHs and $-3.4 - +0.9 \mu\text{g m}^{-2}$
29 d^{-1} for halogenated compounds. Dry particle deposition of FLT and PYR did not contribute
30 significantly to the vertical flux.

31

32 **1. Introduction**

33 The marine atmospheric environment is a receptor for persistent organic pollutants (POPs)
34 which are advected from primary and secondary sources on land, ~~primary and secondary, such~~
35 ~~as volatilization from contaminated soils~~. This is a concern as these substance bioaccumulate
36 along marine food chains (e.g., Lipiatou and Saliot, 1991; Borgå et al., 2001). Primary sources
37 do not exist in the marine environment, except for polycyclic aromatic hydrocarbons (PAHs,
38 ship engines). Long-range transport from urban and industrial sources on land are the
39 predominant sources of PAHs and polychlorinated biphenyls (PCBs) in the global oceans
40 (Atlas and Giam, 1986) and in the Mediterranean (Mandalakis et al., 2005; Tsapakis and
41 Stephanou, 2005; Tsapakis et al., 2006; Iacovidou et al., 2009; Mulder et al., 2015).

42 However, the sea surface itself can turn into a secondary source of POPs provided
43 concentrations build up in surface waters, fed by riverine or atmospheric deposition input.
44 Such studies are still rare. Re-volatilisation was observed for hexachlorocyclohexane (HCH)
45 and PAHs, not only in coastal waters (Lohmann et al., 2011), but also in the open sea
46 (Jantunen and Bidleman, 1995; Lakaschus et al., 2002) including the Mediterranean (Castro-
47 Jiménez et al., 2012; Mulder et al., 2014). After long-term accumulation of declining
48 emissions (even after phase-out), reversal of air-sea exchange may result at some point, as
49 indicated by global modelling for organochlorine pesticides (OCPs; Stemmler and Lammel,
50 2009). The seasonality of on-going emissions on the other hand may trigger a seasonal
51 reversal of air-sea exchange, as indicated for retene, a PAH emitted from biomass burning in
52 the Mediterranean (summer maximum; Mulder et al., 2014). Similarly, PAHs emitted in fossil

53 fuel combustion in residential heating (winter maximum) may re-volatilise seasonally from
54 the sea surface in receptor areas.

55 The direction of diffusive air-surface exchange flux of organics can be identified by
56 comparing the fugacities and can be quantified based on the Whitman two-film model
57 (Bidleman and Connell, 1995; Schwarzenbach et al., 2003) or micro-meteorological
58 techniques. The latter have so far only rarely been used to quantify air-water (Perlinger et al.,
59 2005; Rowe and Perlinger, 2012; Sandy et al., 2012; Wong et al., 2012) or air-soil (Parmele et
60 al., 1972; Majewski et al., 1993; Kurt-Karakus et al., 2006) gas exchange fluxes.

61 We studied the vertical fluxes of POPs at sea surface level with a gradient method at a remote
62 coastal site in the eastern Mediterranean. The measurements were done in the context of a
63 coordinated multi-site campaign on POP cycling in the region (Lammel et al., 2015). The
64 POP concentration in surface seawater was determined, too, such that the direction of air-sea
65 exchange could be addressed by a second method.

66

67 **2.1 Site and sampling**

68 The site selected for atmospheric measurements was Selles Beach, at the northern coast of
69 Crete, 35.2°N/25.4°E, very close (4 km) to the Finokalia observatory. This is a remote site,
70 some 70 km east of major anthropogenic emissions (Iraklion, a city of 100000 inhabitants
71 with airport and industries; Mihalopoulos et al., 1997; Kouvarakis et al., 2000). The
72 Mediterranean region includes urban and industrial areas and is adjacent to ~~to~~-source regions
73 (i.e. western, central and eastern Europe). Exposure of the study area to long-range
74 transported pollution from central and eastern Europe is ~~the~~-highest in summer (Lelieveld et
75 al., 2002).

76 Organic substances were collected 3-13 July in the gaseous and particulate atmospheric
77 phases using low volume samplers ($F \approx 2.3 \text{ m}^3 \text{ h}^{-1}$, Leckel LVS, PM_{10} inlet) equipped with
78 quartz fibre filter (QFF, Whatman QMA 47 mm, baked at 320°C prior to usage) and 2

79 polyurethane foam (PUF) plugs (Molitan, density 0.030 g cm^{-3} , 5.5 cm diameter, total depth
80 10 cm, cleaned by extraction in acetone and dichloromethane, 8 h each) in series. Two of
81 these samplers collected gases and particles at different heights (inlets at $z_1 = 1.05$ and $z_2 =$
82 2.8 m), about 0.5 m apart in the horizontal. According to the Monin-Obukhov similarity
83 theory of turbulent transport in the surface layer (see section S1.3), vertical concentration
84 profiles are expected to be logarithmic, while – due to the vertically non-linear behaviour of
85 the eddy diffusivity – the resulting vertical flux is *per definitionem* constant. For a given
86 surface source (sink) of gases or particles corresponding negative (positive) vertical
87 concentration gradients ($\partial c/\partial z$) will be maximal close to the source (sink). Therefore, over
88 aerodynamically smooth surfaces, the lower inlet height should be preferably in the order of a
89 few tenths of a meter, while the distance to the upper inlet height, should be maximized to
90 yield large (and consequently statistically significant) vertical concentration differences.
91 However, the choice for the upper inlet height is limited by the horizontal extension of the so-
92 called "fetch", i.e. the up-wind surface homogeneity (in terms of orography, structure, and
93 vegetation), which should be at least $100 \times z_2$ (e.g. Foken, 2008). In the case of our study, the
94 choice of the lower inlet height ($z_1=1.05$ m) is just due to the design of the aerosol sampler
95 which does not allow sampling below 1.05 m above ground, while the upper inlet height
96 ($z_2=2.80$ m) accounts for the limited surface homogeneity (200 m) of the Selles Beach site.
97 Day-time (9-20 h EEDST) and night-time (21-8 h EEDST) sampling was conducted from 2
98 July in the evening until 13 July 2012 in the evening. During part of the measurements, from
99 6 July in the morning until 10 July 2012 in the evening, a third sampler was used to collect
100 replica of gaseous samples (PUF plugs only) at z_1 . For the concentration at z_1 , c_{z_1} , replica
101 concentrations (mean of 2 measurements) were used whenever possible. The samplers were
102 placed on a rocky beach. The horizontal distance between the samplers and the water was ≈ 3
103 m, while the vertical distance between the rock and water surfaces was 0.1-0.3 m, varying due

104 to tide and waves. After exposure, filters and PUFs were packed in Al foil and zip-bags,
105 stored and transported in a cool box to the laboratory.

106 Free dissolved contaminants in seawater were sampled using silicone rubber (SR) sheets
107 (Altec, Great Britain) as passive water samplers (PWS). Quantification of trace organics from
108 PWS is sensitive and validated (Rusina et al., 2010). Uncertainties in results obtained by
109 application of partition based passive samplers are believed to range around a factor of two
110 depending on the level of experience of the laboratory (Allan et al., 2009). Different aspects
111 of uncertainty are discussed in Lohmann et al. (2012). At two localities, distanced 0.8 and 2.2
112 km west of Selles Beach, each two SR PWS were deployed in parallel. Each sampler
113 consisted of six sheets ($55 \times 90 \times 0.5$ mm). Before exposure SR sheets were cleaned by
114 Soxhlet extraction in ethyl acetate (96 h) followed by methanol (48 h, shaken), and spiked by
115 a mix of 15 performance reference compounds (PRCs; D₁₀-biphenyl and 13 PCB congeners
116 not occurring in the environment) according to the procedure (Booij et al., 2002). Samplers
117 were deployed 3 July – 2 August 2012 in water mounted on stainless steel wire holders at 1 m
118 depth using buoy and rope. After exposure, samplers were stored and transported in original
119 vials and brought in a cool box to the laboratory.

120 Daily mean temperature was 28.2 (22.4-34.5)°C and wind velocity was 4.8 (0.6-7.7) m s⁻¹
121 (hourly data). No precipitation occurred. The meteorological situation is described in the
122 Supplementary information (SI), S2.1.

123

124 **2.2 Meteorological parameters and vertical flux calculations**

125

126 Boundary layer (BL) depth is needed for interpretation of the variation of the concentrations
127 in air. BL depth data are taken from simulations of the Lagrangian dispersion model
128 FLEXPART, version 9 (Stohl et al., 1998). These were run in forward direction, and based on
129 analysed wind fields (ECMWF, 0.5° resolution). The model BL height is calculated according

130 to Vogelezang and Holtslag (1996) using the critical Richardson number. According to wind
131 direction during sampling we allocate BL depths at upwind locations well off shore (70-100
132 km) or inland (≈ 20 km), respectively, as the relevant BL depth for interpretation of
133 atmospheric concentrations at the coastal site. The mean BL depth during sampling intervals
134 is used.

135 For characterization of the local meteorological conditions, continuous measurements (5 min
136 averages) of air temperature, relative humidity, wind speed and wind direction were accom-
137 plished by three automatic weather stations (model WMT520; Vaisala, Helsinki, Finland)
138 which have been placed at the beach in ≈ 200 m distance (2) and ≈ 100 m inland (1),
139 respectively, from the sampling location. For characterization of the atmospheric surface
140 layer's thermodynamic stratification, vertical profiles of wind speed, wind direction, air tem-
141 perature and relative humidity were determined by continuous measurements at four levels
142 (0.34, 0.70, 1.45, and 3.00 m above ground). Data was recorded by 2D ultrasonic wind
143 sensors (model WMT701; Vaisala, Helsinki, Finland) and aspirated temperature and relative
144 humidity sensors (model MP103A; Rotronic, Bassersdorf, Switzerland) in 10 s intervals,
145 which were averaged to 30 min means for further data processing. For determination of key
146 micrometeorological quantities (e.g., sensible heat flux, friction velocity; see SI, S1.3), fast
147 response measurements of the 3D wind vector and air temperature have been performed by a
148 3D ultrasonic anemometer (CSAT-3, Campbell Scientific Inc., Logan, USA) on a small mast,
149 4 m above ground and about 7 m ESE of the profile mast. Corresponding data were
150 continuously recorded with a sampling frequency of 20 Hz by a suitable logger (model
151 CR3000; Campbell Scientific Inc., Logan, USA). Key micrometeorological quantities were
152 derived from fast response 3D wind and air temperature data (20 Hz) according to the eddy
153 covariance (EC) method; 20 Hz data were processed by the TK3 algorithm (Mauder and
154 Foken, Department of Micrometeorology, University of Bayreuth, Germany), and the results
155 were averaged every 30 minutes. Only periods with wind direction between 270° and 40°

156 (i.e., onshore winds) were considered to calculate vertical fluxes of gaseous organics (more
157 details in the SI, S2.1).

158 The turbulent vertical gaseous organics flux, F_c ($\text{ng m}^{-2} \text{s}^{-1}$), has been calculated according to
159 the aerodynamic method as the product of the vertical difference of concentration, Δc_z (ng m^{-3}),
160 and the turbulent transfer velocity, v_{tr} (m s^{-1}):

$$161 \quad F_c = -v_{\text{tr}} \Delta c_z = -v_{\text{tr}} [c(z_2) - c(z_1)] \quad (1)$$

162
163 where z_2 and z_1 are the heights of inlets of gaseous organics' sampling (1.05 m and 2.80 m,
164 see 2.1, above). The transfer velocity is a measure of the vertical turbulent (eddy) diffusivity.

165 As long as the vertical concentration gradient is statistically significant, and the choice of the
166 upper inlet height accounts for the homogeneity of the up-wind so-called fetch (see above),
167 the resulting flux, calculated from the transfer velocity and the vertical concentration gradient
168 (see eq. (1)), is the vertical turbulent net flux of the corresponding gas, representative for the
169 fetch area and equal to the overall deposition flux (if $c(z_2) - c(z_1) > 0$).

170 Details of the underlying formulation and the calculation scheme are given in the SI, S1.3.

171

172 **2.3 Chemical analysis**

173 For organic analysis all samples were extracted with dichloromethane during ≈ 1 h in an
174 automatic extractor (Büchi B-811). Surrogate extraction standards (D_8 -naphthalene, D_{10} -
175 phenanthrene, D_{12} -perylene, PCB30, PCB185, ^{13}C BDEs 28, 47, 99, 100, 153, 154, 183 and
176 209) were spiked on each PUF and QFF prior to extraction. The volume was reduced after
177 extraction under a gentle nitrogen stream at ambient temperature, and fractionation was
178 achieved on a silica gel column. Samples were analyzed using a GC-MS (gas chromatograph
179 coupled with a mass spectrometer) Agilent 7890 coupled to Agilent 7000B with a J&W

180 Scientific fused silica column DB-5MSUI (60 m × 0.25 mm × 0.25 μm) for 2-4-ring PAHs
181 (naphthalene (NAP), acenaphthylene (ACY), acenaphthene (ACE), fluorene (FLN),
182 phenanthrene (PHE), anthracene (ANT), fluoranthene (FLT), pyrene (PYR),
183 benzo(a)anthracene (BAA), and chrysene (CHR). Terphenyl was used as injection standard.
184 The temperature program was 80°C, 15°C min⁻¹ to 180°C, 5°C min⁻¹ to 310°C. The injection
185 volume was 1 μL in splitless mode at 280°C, with He used as a carrier gas at constant flow of
186 1.5 mL min⁻¹.

187 A sulphuric acid modified silica gel column was used for the PCB/OCP and PBDE cleanup.
188 Samples were analyzed using a GC-MS/MS Agilent 7890 coupled to Agilent 7000B with a
189 SGE HT-8 column (60 m × 0.25 mm × 0.25 μm) for *α*-HCH, *β*-HCH, *γ*-HCH, *δ*-HCH, *o,p'*-
190 and *p,p'*-DDE, -DDD and -DDT, penta- and hexachlorobenzene (PeCB, HCB). PCB 121 was
191 used as injection standard for chlorinated substances. The temperature program was 80°C (1
192 min hold), 40°C min⁻¹ to 200°C, 5°C min⁻¹ to 305°C. The injection volume was 3 μL in
193 splitless mode at 280°C, with He used as a carrier gas at constant flow of 1.5 mL min⁻¹.

194 PBDEs were analysed using GC-HRMS (gas chromatography with high resolution mass
195 spectrometry) on a Restek RTX-1614 column (15 m × 0.25 mm × 0.1 μm). The resolution
196 was set to > 10000 for BDE 28–183, and > 5000 for BDE 209. ¹³C BDEs 77 and 138 were
197 used as injection standards. The MS was operated in EI+ mode at the resolution of >10000.
198 The temperature program was 80°C (1 min hold), then 20°C min⁻¹ to 250°C, followed by
199 1.5°C min⁻¹ to 260°C and 25°C min⁻¹ to 320°C (4.5 min hold). The injection volume was 3 μL
200 in splitless mode at 280°C, with He used as a carrier gas at constant flow of 1 mL min⁻¹.

201
202 Recovery of native analytes varied between 72 and 102% for PAHs, between 88 and 103%
203 for PCBs, and between 75 and 98% for OCPs. The results for PAHs, OCPs and PCBs were
204 not recovery corrected. For PBDEs, isotopic dilution method was used, the average recoveries
205 ranged 78-128%.

206 The mean of 4 field blank values was subtracted from the air sample values. Values below the
207 mean + 3 standard deviations of the field blank values were considered to be <LOQ. Field
208 blank values of most analytes in air samples were below the instrument limit of quantification
209 (ILOQ), which corresponded to 6-34 pg m^{-3} for PAHs, 7-23 pg m^{-3} for PCB and OCPs and
210 0.003-0.04 pg m^{-3} for PBDEs (SI, Table S2). Higher LOQs were determined for analytes in
211 gaseous air samples, namely 0.18 and 0.50 ng m^{-3} for FLN and PHE, and typically 28 pg m^{-3}
212 for HCB. In the particulate phase a higher LOQ resulted for PHE, i.e. 170 pg m^{-3} . The
213 breakthrough in PUF samples was estimated, and as a consequence, NAP, FLN, HCB and
214 PeCB results are not considered as the sampled air volume (typically $\approx 25 \text{ m}^3$ for PUFs)
215 expectedly lead to breakthrough under the prevailing temperatures (Melymuk et al., 2016).
216 Free dissolved water concentrations of analytes in PWS were calculated from amounts
217 accumulated in SRs using the exponential uptake model described in Smedes (2007). The
218 required sampling rates were estimated by fitting performance reference compounds
219 dissipation data from sampler to the model described by Booij and Smedes, 2010. ILOQ
220 corresponded to 0.5-4.2 pg L^{-1} for PAHs (but 9 pg L^{-1} for NAP), 0.05-0.5 pg L^{-1} for PCB and
221 OCPs and 0.0003-0.037 pg L^{-1} for PBDEs (SI, Table S2). Site specific LOQs were 1–10 pg L^{-1}
222 ¹ for PAHs (but 400 pg L^{-1} for NAP), 0.1-0.8 pg L^{-1} for PCB, 0.1–1.4 pg L^{-1} for OCPs (but 2.8
223 pg L^{-1} for α -HCH) and 0.01–0.11 pg L^{-1} for PBDEs (but 0.59 pg L^{-1} for BDE209).

224

225 **2.4 Vertical gradients of trace organics' concentration in air**

226 Air-sea gas exchange can be studied by determining the vertical concentration gradients of
227 trace gases in air (Doskey et al., 2004; Else et al., 2008).

228 Three standard deviations of field blank concentrations are considered as the absolute
229 uncertainty of concentration measurements, c , and twice that much as the uncertainty of
230 concentration differences, Δc_z . Values of concentrations and vertical concentration differences

231 (gradients) not exceeding these thresholds are considered insignificant. This applied for a
232 large fraction of gradients, namely OCP (34 out of 70), PCB (27 out of 44), PBDE (4 out of
233 5), and PAHs (17 out of 46) (Table S3).

234

235 **2.5 Air-water fugacity ratio**

236 The direction of diffusive air-sea gas exchange can be derived from the fugacity ratio
237 calculation, based on the Whitman two-film model (Bidleman and McConnell, 1995). The
238 fugacity ratio, f_a/f_w , is calculated as:

239

$$240 \quad f_a/f_w = c_a R T_a / (c_w H_{T_w, salt}) \quad (2)$$

241

242 with gas-phase concentration c_a (ng m^{-3}), dissolved aqueous concentration c_w (ng m^{-3}),
243 universal gas constant R ($\text{Pa m}^3 \text{ mol}^{-1} \text{ K}^{-1}$), and both sea surface temperature (SST or;
244 T_w ; (K)) and ~~both T_w and~~ salinity corrected Henry's law constant $H_{T_w, salt}$ ($\text{Pa m}^3 \text{ mol}^{-1}$; see
245 S1.1 for details), and air temperature T_a (K). T_a was adopted from the on-site measurement
246 (see above). c_w is derived as the average of the results at two localities, 2 replicas each (see
247 above, 2.1). SST data, measured on the sampling day and in the area, were downloaded from
248 respective database (see S1.4 for details). Air and water sampling was not totally in phase:
249 sampling in air was over 12 days (2-13 July), while SR exposure was during 28 days (3-30
250 July) i.e., collection was done 10 days after air sample collection. Consequently, for those
251 substances which are quickly equilibrated (within a few days) in PWS i.e., HCH and 3-ring
252 PAHs, no simultaneous measurement in air and water was done (see section 2.1). Although
253 the seawater concentrations of HCH and 3-ring PAHs might have been stable over 28 days,
254 no such evidence exists and we refrain from relating the fugacities. Values $0.3 < FR < 3.0$ are
255 conservatively considered to not safely differ from phase equilibrium, as propagating from the
256 uncertainty of the Henry's law constant, $H_{T_w, salt}$, and measured concentrations and

257 temperature changes during sampling (e.g., Bruhn et al., 2003; Castro-Jiménez et al., 2012).
258 Substance property data are taken from the literature (SI, Table S1). This conservative
259 uncertainty margin is also adopted here, while $f_a/f_w > 3.0$ indicates net deposition and f_a/f_w
260 < 0.3 net volatilisation.

261

262 **2.6 Non-steady state 2-box model**

263 The air–sea mass exchange flux of several OCPs and PAHs are simulated by a non-steady
264 state zero-dimensional model of intercompartmental mass exchange (Lammel, 2004; Mulder
265 et al., 2014) in order to test the hypothesis that the diurnal variation of contaminant
266 concentrations in air during a period of on-shore advection of one air mass is explained by the
267 combination of volatilisation from the sea surface and atmospheric mixing depth, while
268 advection (long-range transport) is less significant (horizontal homogeneity of air mass;
269 Lammel et al., 2003). This 2-box model predicts concentrations by integration of two coupled
270 ordinary differential equations that solve the mass balances for the two compartments, namely
271 the atmospheric marine BL and seawater surface mixed layer. Processes considered in air are
272 dry (particle) deposition, removal from air by reaction with the hydroxyl radical, and air-sea
273 mass exchange flux (dry gaseous deposition), while in seawater export (settling) velocity,
274 deposition flux from air, air-sea mass exchange flux (volatilisation), and degradation (as first
275 order process) are considered. Input parameters are listed in the SM, Table S3.

276

277 **3. Results and discussion**

278 **3.1 Day/night variation of concentrations in air**

279 4 PAHs (ACE, PHE, FLT, PYR), 3 OCPs (α - and γ -HCH, p,p' -DDE), 3 PCB congeners
280 (PCB28, -52 and -101) and 2 PBDE congeners (BDE47 and -99) were quantified in gas-phase
281 samples, while the other species were found $< \text{LOQ}$ in all or most samples (Fig. 1a, 2a, Table

282 1a, b). This is a consequence of limited air sample volume ($\approx 25 \text{ m}^3$). PAHs and PBDEs were
283 also found in the particulate phase. The levels observed (Table 1a) are at the lower end of
284 what had been reported from marine, rural and remote sites in the region in the previous ≈ 15
285 years, in particular with regard to the chlorinated species (Kamarianos et al., 2002;
286 Mandalakis and Stephanou, 2002; Tsapakis and Stephanou, 2005; Cetin and Odabasi, 2008;
287 Halse et al., 2011; Lammel et al., 2010 and 2011; Castro-Jiménez et al., 2012; Berrojalbiz et
288 al., 2014; Mulder et al., 2014 and 2015). To our best knowledge, the DDE levels are the
289 lowest reported from the region. This confirms the remote character of the site. Influence of
290 local sources, not expected at this remote site (Iacovidou et al., 2009), is sometimes indicated
291 by an anti-correlation between wind speed and atmospheric concentration. At Selles Beach,
292 dilution by higher wind speed is indeed indicated for one contaminant, ACE (by significant
293 anti-correlation, $p < 0.05$ confidence level, t-test). This is expected, because of its short
294 atmospheric lifetime.

295 BL depths ranged 160-500 m during night-time and 270-760 m during day-time (mean of
296 sampling intervals i.e., 11 h). Day/night variation of contaminants' atmospheric
297 concentrations, often related to mixing and local sources, was not obvious: For PAHs the
298 mean ratio of day/night concentrations (gaseous only), $c_{\text{day}}/c_{\text{night}}$, was ≈ 0.67 (0.54-0.85) for
299 ACE, while $c_{\text{day}}/c_{\text{night}}$ it ranged wider, 0.25-3.35, was $c_{\text{day}}/c_{\text{night}} = 1.4$ - 1.55 for PHE, FLT and
300 PYR, with mean values of $c_{\text{day}}/c_{\text{night}} = 1.41$ -1.53. Also for PBDEs $c_{\text{day}}/c_{\text{night}} > 1$ is found (1.20
301 and 1.37). The low value for ACE can be explained by its short photochemical lifetime (Keyte
302 et al., 2013). $c_{\text{day}}/c_{\text{night}} > 1$ was previously observed for PAHs at the same site and explained
303 by temperature driven volatilisation from surfaces overcompensating for photochemistry (Lee
304 et al., 1998; Tsapakis and Stephanou, 2007). For chlorinated substances, we find mean
305 $c_{\text{day}}/c_{\text{night}} < 1$, namely 0.56-0.66 for HCH isomers, and 0.68-0.945 for PCBs and DDE, while
306 the individual values range widely, 0.04-4.8. However, there was a clear day/night, with
307 mostly night-time maxima of both PAHs (Fig. 1a) and chlorinated species (Fig. 1b)~~trend~~

308 | during a period of continuous on-shore winds, 6-10 July (~~Fig. 1~~). Apparently, contaminants'
309 | concentrations were influenced by BL depth, as indicated by anti-correlation with PAHs and
310 | OCPs (except DDE; significant for α -HCH on the $p < 0.05$ confidence level, t-test). This
311 | results in night-time accumulation. Diel variation~~This~~, apart from mixing, is related to
312 | advection and air-sea mass exchange and studied in more detail in Section 3.2~~5~~.

313

314 | **3.2 Diffusive air-sea exchange**

315 | The variation of air concentrations (with nighttime maxima) during a period of northerly flow
316 | without change of air mass is predicted using the 2-box model (Section 2.6). For PCB28, -52,
317 | FLT and BDE47 air concentrations are qualitatively well captured (Fig. 2, ~~S4~~). These are
318 | maintained by dry gaseous deposition alone (PCB52, FLT) or by oscillating fluxes (HCB,
319 | PCB28: ~~mostly~~ upward, Fig. 2; PYR: mostly downward, Fig. S4a5). The model predicted
320 | fluxes are in good agreement with the observed values (Section 3.3, Table S5) except for each
321 | one day-time sampling interval of FLT and BDE47 (upward fluxes), and for one day-time
322 | interval of PCB28 (downward flux; in total 4 agreements, 3 disagreements). The modelling
323 | results support that (during advection of one air mass) the ~~diurnal~~ variation of contaminant
324 | concentrations in air and, particularly, the night-time accumulation was explained by the
325 | combination of volatilisation from the sea surface and atmospheric mixing depth.
326 | Volatilisation from the sea surface has significantly contributed to the night-time maxima of
327 | HCB (upward flux, Fig. 2) and PCB28 (Fig. 2), as well as of PYR during 1 night (~~night-time~~
328 | ~~upward fluxes~~Fig. S4a; Table S5). This, to our knowledge, had never been observed before.

329 | f_w is derived from the mean concentrations in seawater at two locations (see SI, Table S6, for
330 | individual data). The comparison of air-water fugacity ratios (Section 2.5) suggests for the
331 | measurement period, 2-13 July 2012, net deposition (prevailing downward fluxes, $f_a/f_w > 3$) of
332 | gaseous FLT, PYR, BDE47 and -99, net volatilization (prevailing upward fluxes, $f_a/f_w < 0.3$)
333 | of gaseous PCB28 and -101 and close to phase equilibrium ($0.3 < f_a/f_w < 3$) for p,p' -DDE,

334 and PCB52 (Table 2). These results are the same as determined based on passive air sampling
335 at several locations along the shore at and near Selles Beach (Lammel et al., 2015).
336 The direction of DDE and PCB fluxes derived from fugacity calculations is consistent with
337 what was indicated by the correlation of air concentrations and BL depth during on-shore
338 winds (SI, S2.5).

339

340 **3.3 Vertical concentration gradients in air**

341 PAH vertical gradients mostly indicated deposition, $\Delta c/\Delta z > 0$, found in 28 cases (14 during
342 day, 14 during night), while negative gradients were found in 10 cases (8 during day, 2 during
343 night). The vertical gradient of PAHs was insignificant in 17 cases. When volatilisation was
344 observed (3-5 July for FLT and PYR, 6-9 July for ACE) $\Delta c/\Delta z$ tended to be clearly lower
345 during day-time, indicating that volatilisation of PAHs from the sea surface was stronger
346 during day-time. This could be explained by a higher fugacity from seawater, f_w , which
347 increases with $H_{T_w, salt}$ (see above, 2.5), which, in turn, increases with sea surface temperature,
348 T_w . Similarly, for the halogenated substances, significant positive gradients, $\Delta c/\Delta z > 0$,
349 indicating deposition were more frequent than significant negative gradients i.e., 37 cases (15
350 PCBs, 22 OCPs, 30 during day, 7 during one night only) and 20 cases (2 PCBs, 17 OCPs, 1
351 PBDE, 5 during day, 15 during night), respectively. For these substance classes, a vertical
352 gradient was insignificant in 65 cases (according to the measurement uncertainties). During at
353 least some nights of the period 6-10 July night-time maxima of HCH, and PCB52 in air
354 coincided with negative vertical gradients, i.e. emissions from the sea surface. Diel variation
355 of PCB52 air-sea exchange flux direction is well reflected by the model (Fig. S4b). This
356 trend is most significant for the HCH isomers for which a stronger volatilisation flux from the
357 sea surface is found during the nights than during day time ($\Delta c/\Delta z < 0$), or even deposition
358 during day-time ($\Delta c/\Delta z > 0$ on 6 and 9 July). Hence, volatilisation from the sea surface may

359 have contributed to and may even have caused the night-time maxima of the atmospheric
360 concentrations of HCH and PCB52 (see above and Table 1a): The diel variation of air
361 temperature was small i.e., day-time mean was typically 0.5-1.5 K warmer than night-time
362 mean temperature. Even somewhat lower upward fluxes, F_c , of HCH during night than during
363 day, caused by a slightly lower sea surface temperature, may have caused $c_{\text{day}}/c_{\text{night}} < 1$ in
364 combination with the day/night variation of the BL depth (by average 50% deeper for day-
365 time sampling periods). PBDE day-time maxima may indicate local volatilisation from soil,
366 enhanced during day-time. Again, this is consistent with the positive correlation of air
367 concentrations with BL depth (above). Only one BDE concentration gradient was significant,
368 which was volatilisational and during day-time (Fig. 1b, Table 1b). Fluctuating PCB fluxes
369 are in line with the observation that PCBs were close to phase equilibrium in the Aegean in
370 2006 (Berrojalbiz et al., 2014). Summarizing, average significant day-time vertical gradients,
371 $\Delta c/\Delta z$, of all contaminants exceeded average significant night-time gradients, except for FLT
372 and PYR.

373 The direction of the gradient, hence, of air-sea exchange is found to have changed for ACE,
374 PYR and the HCH isomers on a half-day basis (sequential sampling periods), for FLT during
375 less than 2 days (Table S4). Changing directions of net air-sea mass exchange had been
376 observed in the region along a ship cruise for OCPs, PCBs and one alkylated PAH,
377 dimethylphenanthrene (Castro-Jiménez et al., 2012; Berrojalbiz et al., 2014) in 2006 and for
378 FLT and PYR in 2010 (Mulder et al., 2014). Fast fluctuation of the direction of air-sea
379 exchange throughout large parts of the year had been found for one alkylated PAH, retene, in
380 the sea region following biomass burning emissions (based on box modelling; Mulder et al.,
381 2014). Earlier, in 2000-02 air-sea exchange of PAHs was found depositional for all members
382 (Tsapakis et al., 2006).

383 These observations of an increasing number of pollutants attaining phase equilibrium and bi-
384 directional flux may indicate a long-term trend from deposition towards 'reversal', i.e.

385 volatilisation of these pollutants in the marine environment of the eastern Mediterranean and,
386 more general, of receptor seas regions, located in the outflow of regions emitting long-lived
387 semivolatile pollutants, such as most POPs. For substances close to phase equilibrium
388 (attained in a long-term trend) the direction of air-sea exchange may change with a high
389 frequency, as found here. Implicitly, dry deposition is difficult to budget. However,
390 fluctuation may also occur in response to seasonal trends: In summer 2010 FLT and PYR
391 were found close to phase equilibrium in the eastern Mediterranean, while retene (RET) was
392 found mostly volatilisational. A model simulation had revealed that seasonal primary
393 emissions and subsequent deposition of RET (from open fires in the region) are triggering
394 seasonal flux reversal, which over many weeks, however, is fluctuating with a high frequency
395 (< 24 h). (Mulder et al., 2014) Obviously, longer observations are needed to assess the
396 prevailing vertical flux direction. Extrapolation of the observations to annual fluxes is not
397 justified, as day/night fluctuations may be part of a more complex temporal pattern. The
398 seawater surface as secondary source of pollution should be assessed based on flux
399 measurements during several seasons and over longer time periods.

400

401 **3.4 Quantification of vertical fluxes of gaseous contaminants**

402 Vertical fluxes, F_c , can be quantified for periods with transfer velocity, v_{tr} , determined, which
403 varied between 3.3 and 8.4 cm s^{-1} , by average it was $5.3 \pm 1.9 \text{ cm s}^{-1}$. The time coverage of this
404 parameter was 70%, however, i.e., satisfying time coverage of sampling intervals was
405 achieved during 14 out of 20 sampling intervals, 11 days (by average 5.5 cm s^{-1}) and 3 nights
406 (by average 3.5 cm s^{-1}) (Figures 1a, 2c, Table S5).

407 The fluxes of PAHs could be determined based on 8 periods of day-time and 2 periods of
408 night-time sampling. 15 PAH fluxes were downward ($F_c = -3.6 \pm 7.0 \mu\text{g m}^{-2} \text{ d}^{-1}$), 8 upward
409 (ranging $F_c = 0.8 \pm 0.6 \mu\text{g m}^{-2} \text{ d}^{-1}$) and insignificant ($|F_c| < (0.7 \pm 0.7) \mu\text{g m}^{-2} \text{ d}^{-1}$) in 13 cases.

410 Both directions were observed for 3 species, while the flux of PHE was downward (by
411 average $F_c = -7.3 \mu\text{g m}^{-2} \text{d}^{-1}$) whenever significant (Table S5a). With

412

413 $v_{\text{dep}} = -F_c / c_g$ (3);

414

415 this corresponded to a mean deposition velocity for gaseous PHE of $v_{\text{dep}} = 0.0043 \pm 0.0031 \text{ cm}$
416 s^{-1} , still significantly deviating from zero (1 standard deviation criterion, based on
417 measurement at $z_1 = 1.05 \text{ m}$). Even 3-ring PAHs' deposition is dominated by the particulate
418 phase and a wide range has been reported ($0.001\text{-}10 \text{ cm s}^{-1}$; Zhang et al., 2015), also based on
419 measurements in the region (Tasdemir and Esen, 2009). During the first days of the campaign
420 FLT and PYR were volatilised, later deposited, too.

421 For 11 periods of day-time and 2 of night-time sampling the fluxes of 8 halogenated
422 substances were downward in 12 cases ($F_c = -0.58 \pm 0.87 \mu\text{g m}^{-2} \text{d}^{-1}$), upward in 6 cases ($F_c =$
423 $0.30 \pm 0.31 \mu\text{g m}^{-2} \text{d}^{-1}$; these were 0.11-0.25 for γ -hexachlorocyclohexane (HCH) and $0.91 \mu\text{g}$
424 $\text{m}^{-2} \text{d}^{-1}$ for BDE47) and insignificant in 15 cases ($|F_c| \lesssim 0.19 \pm 0.45 \mu\text{g m}^{-2} \text{d}^{-1}$) (Table S5b).

425 The fluxes corresponded to mean deposition velocities not distinguishable from zero e.g.,
426 $0.020 \pm 0.032 \text{ cm s}^{-1}$ for α -HCH and $0.011 \pm 0.015 \text{ cm s}^{-1}$ for PCB28 (1 standard deviation
427 criterion).

428 Air-sea exchange fluxes had been estimated earlier based on measurements in air and
429 seawater in the Aegean Sea and application of the 2-film model for PAHs in 2001-02
430 (Tsapakis et al., 2006) and in spring 2006 for PAHs, HCB and PCBs (Castro-Jiménez et al.,
431 2012). Hereby, the flux is calculated proportional to a substance specific mass transfer
432 coefficient, k_{ol} , strongly dependent on wind velocity and sea surface temperature (Jurado et
433 al., 2004; Mandalakis et al., 2005). For both PCBs and PAHs widely varying k_{ol} values have
434 been estimated (Gigliotti et al., 2002; Mandalakis et al., 2005). The corresponding mean F_c (5
435 sampling periods, just 1 in the case of ACE; Table S5) found in our study, 2012, has the same

436 direction but exceeds by more than one and two orders of magnitude, respectively, the
437 previous findings for PHE (downward) and FLT (downward in 2001-02, upward in 2006). For
438 PYR the opposite direction (now upward, downward in 2001-02 and 2006) is found. The flux
439 direction found for the PCBs is unchanged compared to the 2006 measurements, then found
440 close to phase equilibrium (Berrojalbiz et al., 2014).

441

442 **3.5 Particulate phase concentrations and total deposition**

443 Only PAHs and PBDEs were found exceeding LOQ in the particulate phase. Their day-night
444 variation was minimal (Table S3a, b), by average $c_{\text{day}}/c_{\text{night}} = 0.90-1.18$ for particulate PAHs,
445 1.03 and 1.07 for the PBDEs. This supports the perception that particulate PAH is not
446 attacked by the hydroxyl radical, but ‘shielded’ by the particle matrix (e.g. Zhou et al., 2012).

447 The same had been observed previously at the same site (Tsapakis and Stephanou, 2007).

448 | Effective photochemistry can also be excluded for particulate PBDEs for the same reason.

449 | While $c_{\text{day}}/c_{\text{night}} = 1.20$ and 1.37 for gaseous PBDEs suggests volatilisation from ground
450 during the day, the absence of $c_{\text{day}}/c_{\text{night}} > 1$ for the particulate phase may indicate that the
451 species are not in gas-particle phase equilibrium. This has been pointed out based on previous
452 PBDE measurements in the region (Cetin and Odabasi, 2008). However, the data set
453 discussed here is limited and gas-particle partitioning was not the subject of this study.

454 Total deposition is the sum of dry and wet deposition, the latter not being significant in the
455 | Mediterranean in summer, because of small amount of precipitation. Dry deposition is the
456 | sum of particle deposition and diffusive depositional fluxes (part of air-sea exchange, see 3.2).

457 The dry particle deposition flux, $F_{p \text{ dep}}$, can be estimated based on

458

459 |
$$F_{p \text{ dep}} = -v_{\text{dep}} C_p \tag{4}$$

460

461 with v_{dep} being determined by particle size and wind speed and c_p determined close to the sea
462 surface. Dry particle deposition to the sea surface is most efficient under high wind speeds
463 (Williams, 1982). The mass median diameter of PAHs at remote sites has been mostly found
464 in the submicrometer range (Lipiatou and Saliot, 1991), also during the measurements
465 reported here (own, unpublished data measured simultaneously). For particles of $0.5 \mu\text{m}$
466 aerodynamic size $v_{\text{dep}} \approx 0.1 \text{ cm s}^{-1}$ can be expected for the mean wind velocity at Selles
467 Beach, i.e. 5 m s^{-1} . ~~Actually, v_{dep} is not very sensitive to wind speed for this particle size~~
468 ~~range~~. (Slinn and Slinn, 1980). Adopting $v_{\text{dep}} = 0.1 \text{ cm s}^{-1}$ would suggest $F_{\text{p dep}} \approx -0.023$, -
469 0.016 and $-0.010 \mu\text{g m}^{-2} \text{ d}^{-1}$ for PHE, FLT and PYR ($c_p = 0.26$, 0.19 and 0.11 ng m^{-3} ,
470 respectively, mean of the same 5 day-time sampling intervals in the period 3-10 July for
471 which F_c was determined, Table S5a). This means that the contribution of $F_{\text{p dep}}$ to dry
472 deposition of PHE was negligible ($F_{\text{cp-dep}} \approx 1000 \times F_{\text{p dep}}$; $F_c = -26 \mu\text{g m}^{-2} \text{ d}^{-1}$) and $F_{\text{p dep}}$
473 negligibly compensated for net-volatilization of FLT and PYR in diffusive air-sea exchange (F_c
474 $= +0.91$ and $+0.79 \mu\text{g m}^{-2} \text{ d}^{-1}$ for FLT and PYR, respectively). The values of v_{dep} integrated
475 over the entire size spectrum may differ considerably from values of v_{dep} for MMD (Ruijgrok
476 et al., 1995). Furthermore, the mass median diameter of the semivolatile PAHs FLT and PYR
477 might well be larger than $0.5 \mu\text{m}$ as a consequence of redistribution in the aerosol along
478 transport. However, even then, particle deposition ~~is unlikely to~~~~could not~~ have significantly
479 compensated for net-volatilization, as even for $1 \mu\text{m}$ particles grown to $1.5 \mu\text{m}$ $F_{\text{p dep}}$
480 would be higher by ~~not more than~~~~approximately~~ a factor of ~~103~~ (Slinn and Slinn, 1980). For
481 PHE, FLT and PYR $F_{\text{p dep}} = -0.021$, -0.018 and $-0.009 \mu\text{g m}^{-2} \text{ d}^{-1}$, respectively, were
482 determined experimentally at Finokalia Observatory in 2001 (mean of 25 weeks between
483 March and October; Tzapakis et al., 2006). This means that within measurement uncertainties
484 the particle deposition fluxes found in 2012 are the same than one decade earlier, in both
485 absolute and relative (3 PAH members) terms. These fluxes are also in agreement with what

486 was estimated in the Aegean Sea in summer 2006, namely $F_{p\text{ dep}} = -0.010\text{--} -0.015 \mu\text{g m}^{-2} \text{d}^{-1}$
487 for the same PAHs based on assuming $v_{\text{dep}} \approx 0.2 \text{ cm s}^{-1}$ (Castro-Jiménez et al., 2012).

488 A similar calculation ~~of~~ for the BDEs for one day-time sampling interval ($c_p = 0.16$ and 0.20
489 ng m^{-3} for BDE47 and BDE99, respectively, 6 July for which F_c was determined, Table S5b)
490 suggests that the contribution of $F_{p\text{ dep}}$ to dry deposition of BDE47 was negligible, too ($F_{\text{cp-dep}}$
491 $\approx 100 \times F_{p\text{ dep}}$; $F_c = +3.0 \mu\text{g m}^{-2} \text{d}^{-1}$), while no direct comparison can be made for BDE99
492 ($|F_c| \leq 3.8 \mu\text{g m}^{-2} \text{d}^{-1}$; Table S5b). Hereby, $v_{\text{dep}} = 0.05\text{--}0.3 \text{ cm s}^{-1}$ was adopted to account for
493 mass median diameters ranging 0.5-1.5 ~~close to 1 μm near the sources~~ and mass transfer
494 kinetic limitations for re-distribution during long-range transport (Cetin and Odabasi, 2008;
495 Luo et al., 2014; and in agreement with own, unpublished data measured simultaneously in a
496 short distance).

497 Significant vertical concentration differences in the particulate phase, $\Delta c_p / \Delta z > 0$ and $\Delta c_p / \Delta z$
498 < 0 , were found. Notably during one day-time and sequential night-time sampling (6-7 July)
499 and during day-time of 9 July all significant gradients determined for particulate phase
500 contaminants were negative, i.e. higher concentrations at the lower level, z_1 (PHE and FLT
501 each 1, PYR 2 cases; PBDEs each 1 case; Table S3), while the opposite gradient was found in
502 other nights and days. Marine aerosol contains organic matter (OM), mostly in the
503 accumulation mode, in particular over biological productive surface waters and under low
504 wind speeds (Gantt et al., 2011; Albert et al., 2012). A considerable part of OM is water
505 insoluble (O'Dowd et al., 2004; Facchini et al., 2008). Hence, the marine aerosol contains
506 traces of POPs, which previously were in either dissolved form or associated with suspended
507 OM. ~~Apart from particle sources at the ground (not relevant here), v~~Vertical particle gradients
508 may be sustained by turbulent diffusion (Pryor et al., 2008). While average wind speed was
509 highest during day-time of 9 July, it was average during 6-7 July. No fluxes can be derived
510 from the gradients determined in this study, downward or upward.

511

512 4. Conclusions

513 The diurnal variation of contaminant concentrations in air at a remote coastal site in the
514 Aegean Sea was explained by the combination of atmospheric mixing depth and volatilisation
515 from the sea surface. Volatilisation from the sea surface has significantly contributed to the
516 night-time maxima of (at least) HCB, HCH, PCB28, PCB52 and PYR/PCB28. Apart from
517 long-range transport across the Aegean Sea, local sources were indicated for PBDEs: PBDE
518 cycling was characterized by volatilization and transport from the island during the day and
519 deposition to the sea surface.

520 We successfully quantified the diffusive air-sea exchange flux of 4 3-4 ring PAHs (in the
521 upper pg m^{-3} concentration range), 3 OCPs, 3 PCBs and 2 PBDEs (in the lower pg m^{-3}
522 concentration range) at a remote coastal site using a gradient in combination with the eddy
523 covariance technique. Many vertical gradients were insignificant and concentrations of other
524 analytically targeted PAHs, PCBs, OCPs and PBDEs remained <LOQ. More substances could
525 have been included using high-volume sampling, by which the sampled air volume could
526 have been increased by one order of magnitude.

527 Both flux directions were observed (fluctuation) for the OCPs studied, as well as for 3 PAHs
528 (ACE, FLT, PYR) and 1 PCB (PCB52), not determined by the day-night cycle. Fluctuation of
529 more substances addressed might have been hidden by ~~the~~ gaps in the time series of fluxes
530 (limited by the uncertainties of sampling and analysis) or the time resolution (limited by the
531 sensitivity of the analytical method)method's uncertainties. Hence, the mean flux direction on
532 one hand side and observations during part of the time of the trace substances may differ. E.g.
533 volatilisation of BDE47 (observed in 1 night only) may have been the exception. In general,
534 longer observations and across seasons of the flux is needed to assess dry deposition fluxes
535 and the state of air-sea exchange of those anthropogenic trace substances, which have been

536 approaching phase equilibrium historically (Jantunen and Bidleman, 1995; Stemmler and
537 Lammel, 2009; Berrojalbiz et al., 2014) or seasonally (Mulder et al., 2014).

538

539 **Acknowledgements**

540 We thank Giorgos Kouvarakis and Nikolas Mihalopoulos, University of Crete, Iraklion, and
541 Günter Schebeske, MPIC, for on-site support and Dušan Lago, MU, for air mass back-
542 trajectory modelling. This research was supported by the Granting Agency of the Czech
543 Republic (project No. 312334), the Czech Ministry of Education, [Youth and Sports \(LO1214](#)
544 [and LM2015051\)](#), and the European Union FP7 (~~No. under grant agreement n^o 262254,~~
545 ~~(ACTRIS)~~).

546

547 **Supporting Information**

548 Detailed methodological information (substance properties, analytical quality assurance
549 parameters, micrometeorological technique, two-box model) and results (meteorological
550 situation, transfer velocity, atmospheric concentration and flux data).

551

552 **References**

553 [Albert, M.F.M.A., Schaap, M., Manders, A.M.M., Scannell, C., O'Dowd, C.D., and de](#)
554 [Leeuw, G.: Uncertainties in the determination of global sub-micron marine organic matter](#)
555 [emissions. *Atmos. Environ.*, 57, 289-300, 2012.](#)

556 Allan, I.J., Booij, K., Paschke, A., Vrana, B., Mills, G.A., and Greenwood, R.: Field
557 performance of seven passive sampling devices for monitoring of hydrophobic substances.
558 *Environ. Sci. Technol.*, 43, 5383-5390, 2009.

559 Atlas, E., and Giam, C.S.: Sea-air exchange of high-molecular weight synthetic organic
560 compounds. In: *The role of air-sea exchange in geochemical cycles* (Buat-Ménard, P.,
561 ed.), NATO ASI Ser. Vol. C185, Reidel, Dordrecht, the Netherlands, pp. 295-329, 1986

562 Berrojalbiz, N., Castro-Jiménez, J., Mariani, G., Wollgast, J., Hanke, G., and Dachs, J.:
563 Atmospheric occurrence, transport and deposition of polychlorinated biphenyls and
564 hexachlorobenzene in the Mediterranean and Black Seas. *Atmos. Chem. Phys.*, 14, 8947-
565 8959, 2014.

566 Bidleman, T.F., and McConnell, L.L.: A review of field experiments to determine air-water
567 gas-exchange of persistent organic pollutants. *Sci. Total Environ.*, 159, 101-107, 1995.

568 Booij, K., and Smedes, F.: An improved method for estimating in situ sampling rates of
569 nonpolar passive samplers. *Environ. Sci. Technol.*, 44, 6789-6794, 2010.

570 Borgå, K., Gabrielsen, G.W., and Skaare, J.U.: Biomagnification of organochlorines along a
571 Barents Sea food chain. *Environ. Pollut.*, 113, 187-198, 2001.

572 Bruhn, R., Lakaschus, S., and McLachlan, M.S.: Air/sea gas exchange of PCBs in the
573 southern Baltic sea. *Atmos. Environ.*, 37, 3445-3454, 2003.

574 Castro-Jiménez, J., Berrojalbiz, N., Wollgast, J., and Dachs, J.: Polycyclic aromatic
575 hydrocarbons (PAHs) in the Mediterranean Sea: Atmospheric occurrence, deposition and
576 decoupling with settling fluxes in the water column. *Environ. Pollut.*, 166, 40-47, 2012.

577 Cetin, B., and Odabasi, M.: Atmospheric concentrations and phase partitioning of
578 polybrominated diphenyl ethers (PBDEs) in Izmir, Turkey. *Chemosphere*, 71, 1067-1078,
579 2008.

580 Doskey, P.V., Kotamarthi, V.R., Fukui, Y., Cook, D.R., Breitbeil, F.W., and Wesely, M.L.:
581 Air-surface exchange of peroxyacetyl nitrate at a grassland site. *J. Geophys. Res.*, 109,
582 D10310, 2004.

583 Else, B.G.T., Papakyriakou, T.N., Granskog, M.A., and Yackel, J.J.: Observations of sea
584 surface f_{CO_2} distributions and estimated air–sea CO_2 fluxes in the Hudson Bay region
585 (Canada) during the open water season. *J. Geophys. Res.*, 113, C08026, 2004.

586 [Facchini, M.C., Rinaldi, M., Decesari, S., Carbone, C., Finessi, E., Mircea, M., Fuzzi, S.,
587 Ceburnis, D., Flanagan, R., Nilsson, E.D., de Leeuw, G., Martino, M., Woeltjen, J., and
588 O’Dowd, C.D.: Primary submicron marine aerosol dominated by insoluble organic
589 colloids and aggregates, *Geophys. Res. Lett.*, 35, L17814, 2008.](#)

590 [Foken, T., 2008. *Micrometeorology*, Springer, Heidelberg, 308 pp.](#)

591 [Gantt, B., Meskhidze, N., Facchini, M.C., Rinaldi, M., Ceburnis, D., and O’Dowd, C.D.,
592 2011. Wind speed dependent size-resolved parameterization for the organic mass fraction
593 of sea spray aerosol. *Atmos. Chem. Phys.*, 11, 8777-8790, 2011.](#)

594 Gigliotti, C.L., Brunciak, P.A., Dachs, J., Glenn, T.R., Nelson, E.D., Totten, L.A., and
595 Eisenreich, S.J.: Air-water exchange of polycyclic aromatic hydrocarbons in
596 theNewYork-NewJersey, USA, harbor estuary. *Environ. Toxicol. Chem.*, 21, 235-244,
597 2002.

598 Halse, A.K., Schlabach, M., Eckhardt, S., Sweetman, A.J., Jones, K.C., and Breivik, K.:
599 Spatial variability of POPs in European background air. *Atmos. Chem. Phys.*, 11, 1549–
600 1564, 2011.

601 Jantunen, L.M., and Bidleman, T.F.: Reversal of the air-water gas-exchange direction of
602 hexachlorocyclohexanes in the Bering and Chukchi Seas: 1993 vs. 1988, *Environ. Sci.*
603 *Technol.*, 29, 1081-1089, 1995.

604 Kamarianos, A., Karamanlis, X., and Galoupi, E.: Pollution of coastal areas of N. Greece by
605 organochlorine pesticides and polychlorinated biphenyls (PCBs). In: Proceedings of the
606 1st Environmental Conference of Macedonia, 1–4 March 2002, Thessaloniki, Greece, pp.
607 116–121, 2002.

608 Keyte I.J., Harrison R.M., and Lammel G.: Chemical reactivity and long-range transport
609 potential of polycyclic aromatic hydrocarbons – a review. *Chem. Soc. Rev.*, 42, 9333-
610 9391, 2013.

611 Kouvarakis, G., Tsigaridis, K., Kanakidou, M., and Mihalopoulos, N.: Temporal variations of
612 surface regional background ozone over Crete Island in the southeast Mediterranean. *J.*
613 *Geophys. Res.*, 105, 4399-4407, 2000.

614 Kurt-Karakus, P.B., Bidleman, T.F., Staebler, R.M., and Jones, K.C.: Measurement of DDT
615 fluxes from a historically treated agricultural soil in Canada, *Environ. Sci. Technol.*, 40,
616 4578-4585, 2006.

617 Lakaschus, S., Weber, K., Wania, F., and Schrems, O.: The air-sea equilibrium and time trend
618 of hexachlorocyclohexanes in the Atlantic Ocean between the Arctic and Antarctica,
619 *Environ. Sci. Technol.*, 36, 138– 145, 2002.

620 Lammel, G., Brüggemann, E., Müller, K., and Röhr, A.: On the horizontal homogeneity of
621 mass-related aerosol properties, *Environ. Monitoring Assessment*, 84, 265-273, 2003.

622 Lammel, G., Klánová, J., Ilić, P., Kohoutek, J., Gasić, B., Kovacić, I., Lakić, N., and Radić,
623 R.: Polycyclic aromatic hydrocarbons on small spatial and temporal scales – I. Levels and
624 variabilities. *Atmos. Environ.*, 44, 5015-5021, 2010.

625 Lammel, G., Klánová, J., Erić, L., Ilić, P., Kohoutek, J., and Kovacić, I.: Sources of
626 organochlorine pesticides in an urban Mediterranean environment: Volatilisation from
627 soil, *J. Environ. Monit.*, 13, 3358–3364, 2011.

628 Lammel, G., Audy, O., Besis, A., Efstathiou, C., Eleftheriadis, K., Kohoutek, J., Kukučka, P.,
629 Mulder, M.D., Příbylová, P., Prokeš, R., Rusina, T., Samara, C., Sofuoglu, A., Sofuoglu,
630 S.C., Tasdemir, Y., Vassilatou, V., Voutsas, D., and Vrana B.: Air and seawater pollution
631 and air-sea exchange of persistent organic pollutants in the Aegean Sea: spatial trends of
632 PAHs, PCBs, OCPs and PBDEs. *Environ. Sci. Pollut. Res.*, 22, 11301-11313, 2015.

633 Lee, R.G.M., Hung, H., Mackay, D., and Jones, K.C. : Measurement and modeling of the
634 diurnal cycling of atmospheric PCBs and PAHs. *Environ. Sci. Technol.*, 32, 2172-2179,
635 1998.

636 Lipiatou, E., Saliot, A. : Fluxes and transport of anthropogenic and natural polycyclic
637 aromatic-hydrocarbons in the western Mediterranean Sea. *Mar. Chem.*, 32, 51-71. , 1991.

638 Lohmann, R., Dapsis, M., Morgan, E.J., Dekany, E., and Luey, P.J.: Determining air-water
639 exchange spatial and temporal trends of freely dissolved PAHs in an urban estuary using
640 passive polyethylene samplers. *Environ. Sci. Technol.*, 45, 2655-2662, 2011.

641 Lohmann, R., Booij, K., Smedes, F., and Vrana, B.: Use of passive sampling devices for
642 monitoring and compliance checking of POP concentrations in water. *Environ. Sci. Pollut.*
643 *Res.*, 19, 1885-95, 2012.

644 Luo, P., Ni, H.G., Bao, L.J., Li, S.M., and Zeng, E.Y.: Size distribution of airborne particle-
645 bound polybrominated diphenyl ethers and its implications for dry and wet deposition.
646 *Environ. Sci. Technol.*, 48, 13793-13799, 2014.

647 Majewski, M.S., Desjardins, R., Rochette, P., Pattey, E., Seiber, J., and Glotfelty, D.E.: Field
648 comparison of an eddy accumulation and an aerodynamic-gradient system for measuring
649 pesticide volatilization fluxes. *Environ. Sci. Technol.*, 27, 121-128, 1993.

650 Mandalakis, M., and Stephanou, E.G.: Study of atmospheric PCB concentrations over eastern
651 Mediterranean Sea. *J. Geophys. Res.*, 107, 4716, 2002.

652 Mandalakis, M., Apostolaki, M., Stephanou, E.G., and Stavrakakis, S.: Mass budget and
653 dynamics of polychlorinated biphenyls in the east Mediterranean Sea. *Glob. Biogeochem.*
654 *Cycles*, 19, GB3018, 2005.

655 Melymuk, L., Bohlin-Nizzetto, P., Prokeš, R., Kukučka, P., and Klánová, J.: Sampling
656 artifacts in active air sampling of semivolatile organic contaminants: Comparing
657 theoretical and measured artifacts and evaluating implications for monitoring networks.
658 *Environ. Pollut.* doi:10.1016/j.envpol.2015.12.015, 2016.

659 Mihalopoulos, N., Stephanou, E., Pilitsidis, S., Kanakidou, M., and Bousquet, P.:
660 Atmospheric aerosol composition above the Eastern Mediterranean region. *Tellus B*, 49,
661 314-326, 1997.

662 Mulder, M.D., Heil, A., Kukučka, P., Klánová, J., Kuta, J., Prokeš, R., Sprovieri, F., and
663 Lammel, G.: Air-sea exchange and gas-particle partitioning of polycyclic aromatic
664 hydrocarbons in the Mediterranean. *Atmos. Chem. Phys.*, 14, 8905-8915, 2014.

665 Mulder, M.D., Heil, A., Kukučka, P., Kuta, J., Příbylová, P., Prokeš, R., and Lammel, G.:
666 Long-range atmospheric transport of PAHs, PCBs, OCPs and PBDEs to the central and
667 eastern Mediterranean 2010. *Atmos. Environ.*, 111, 51-59, 2015.

668 [O'Dowd, C.D., Facchini, M.C., Cavalli, F., Ceburnis, D., Mircea, M., Decesari, S., Fuzzi, S.,](#)
669 [Yoon, Y.J., and Putaud, J.P.: Biogenically driven organic contribution to marine aerosol.](#)
670 [Nature, 431, 676-680, 2004.](#)

671 Parmele, L.H., Lemon, E.R., and Taylor, A.W.: Micrometeorological measurement of
672 pesticide vapor flux from bare soil and corn under field conditions. *Water Air Soil Pollut.*,
673 1, 433-451, 1972.

674 Perlinger, J.A., Tobias, D.E., Morrow, P.S., and Doskey, P.V.: Evaluation of novel techniques
675 for measurement of air-water exchange or persistent bioaccumulative toxicants in Lake
676 Superior. *Environ. Sci. Technol.*, 39, 8411-8419, 2005.

677 Rowe, M.D., and Perlinger, J.A.: Micrometeorological measurement of hexachlorobenzene
678 and polychlorinated biphenyl compound air-water gas exchange in Lake Superior and
679 comparison to model predictions. *Atmos. Chem. Phys.*, 12, 4607-4617, 2012.

680 [Ruijgrok, W., Davidson, C.I., and Nicholson, K.W.: Dry deposition of particles – implications](#)
681 [and recommendations for mapping of deposition over Europe. Tellus B, 47, 587-601,](#)
682 [1995.](#)

683 Rusina, T., Smedes, F., Kobližková, M., and Klánová, J.: Calibration of silicone rubber
684 passive samplers: experimental and modeled relations between sampling rate and
685 compound properties. *Environ. Sci. Technol.*, 44, 362-367, 2010a.

686 Rusina, T., Smedes, F., and Klanova, J.: Diffusion coefficients of polychlorinated biphenyls
687 and polycyclic aromatic hydrocarbons in polydimethylsiloxane and low-density
688 polyethylene polymers. *J. Appl. Polymer Sci.*, 116, 1803-1810, 2010b.

689 Sandy, A.L., Guo, J., Miskewitz, R.J., McGillis, W.R., and Rodenburg, L.A.: Fluxes of
690 polychlorinated biphenyls volatilizing from the Hudson River, New York measured using
691 micrometeorological approaches. *Environ. Sci. Technol.*, 46, 885-891, 2012.

692 Schwarzenbach, R.P., Gschwend, P.M., and Imboden, D.M.: *Environmental Organic*
693 *Chemistry*, 2nd ed., Wiley, Hoboken, USA, 2003.

694 Slinn, S.A., and Slinn, W.G.N.: Predictions for particle deposition on natural waters. *Atmos.*
695 *Environ.*, 14, 1013-1016, 1980.

696 Smedes, F.: Monitoring of chlorinated biphenyls and polycyclic aromatic hydrocarbons by
697 passive sampling in concert with deployed mussels. In: *Passive sampling techniques in*
698 *Environmental Monitoring (Comprehensive Analytical Chemistry Vol. 48; Greenwood,*
699 *R., Mills, G., Vrana, B., eds.), pp. 407–448, Elsevier, Amsterdam, the Netherlands, 2007.*

700 Stemmler, I., and Lammel, G.: Cycling of DDT in the global oceans 1950-2002: World ocean
701 returns the pollutant. *Geophys. Res. Lett.*, 36, L24602, 2009.

702 Stohl, A., Hittenberger, M., and Wotawa, G.: Validation of the Lagrangian particle dispersion
703 model FLEXPART against large scale tracer experiments. *Atmos. Environ.*, 32, 4245-
704 4264, 1998.

705 Tasdemir, Y., and Esen, F.: Dry deposition fluxes and deposition velocities of PAHs at an
706 urban site in Turkey. *Atmos. Environ.*, 41, 1288-1301, 2007.

707 Tsapakis, M., and Stephanou, E.G.: Polycyclic aromatic hydrocarbons in the atmosphere of
708 the Eastern Mediterranean. *Environ. Sci. Technol.*, 39, 6584-6590, 2005.

709 Tsapakis, M., and Stephanou, E.G.: Diurnal cycle of PAHs, nitro-PAHs and oxy-PAHs in a
710 high oxidation capacity marine background atmosphere. *Environ. Sci. Technol.*, 41, 8011-
711 8017, 2007.

712 Tsapakis M., Apostolaki, M., Eisenreich, S., and Stephanou, E.G.: Atmospheric deposition
713 and marine sediment fluxes of polycyclic aromatic hydrocarbons in the east
714 Mediterranean Basin. *Environ. Sci. Technol.* 40, 4922-4927, 2006.

715 UNEP-GEMS - United Nations Environment Programme Global Environment Monitoring
716 System: Water Programme, annual report, Geneva, 2006.

717 Vogelezang, D.H.P., and Holtslag, A.A.M.: Evaluation and model impacts of alternative
718 boundary-layer height formulations. *Bound. Layer Met.*, 81, 245–269, 1996.

719 Williams, R.M.: A model for the dry deposition of particles to natural water surfaces. *Atmos.*
720 *Environ.*, 16, 1933-1938, 1982.

721 Wong, F., Jantunen, L.M., Papakyriakou, T., Staebler, R.M., Stern, G.A., and Bidleman, T.F.:
722 Comparison of micrometeorological and two-film estimates of air-water gas exchange for
723 α -hexachlorocyclohexane in the Canadian Archipelago. *Environ. Sci. Pollut. Res.*, 19,
724 1908-1914, 2012.

725 Zhang, L.M., Cheng, I., Wu, Z.Y., Harner, T., Schuster, J., Charland, J.P., Muir, D., and
726 Parnis, J.M.: Dry deposition of polycyclic aromatic compounds to various land covers in
727 the Athabasca oil sands region. *J. Adv. Model. Earth Syst.*, 7, 1339-1350, 2015.

728 Zhou, S., Lee, A.K.Y., McWhinney, R.D., and Abbatt, J.P.D.: Burial effects of organic
729 coatings on the heterogeneous reactivity of particle-borne benzo(a)pyrene (BaP) towards
730 ozone. *J. Phys. Chem. A*, 116, 7050-7055, 2012.

731 Table 1. Statistics of (a) concentrations at ground level, $z_1 = 1.05$ m and (b) vertical gradients,
 732 Δc_z , over $\Delta z = 1.75$ m of gaseous PAHs and halogenated POPs. Mean \pm standard deviation (n,
 733 min-max), ng m^{-3} , except PBDEs: pg m^{-3}). All data included (exceeding or below uncertainty
 734 thresholds), individual data: see Tables S3, S4. For mean and standard deviations values
 735 $<$ LOQ were replaced by LOQ/2.

736 a.

| | all samples | night-time | day-time |
|------------------|---------------------------------|------------------------------------|-------------------------------------|
| ACE | 0.091 \pm 0.021 (0.059–0.12) | 0.11 \pm 0.006 (5, 0.11–0.12) | 0.076 \pm 0.012 (5, 0.059–0.091) |
| PHE | 1.28 \pm 0.89 (0.21–3.54) | 1.00 \pm 0.52 (8, 0.21–1.46) | 1.47 \pm 1.10 (10, 0.25–3.54) |
| FLT | 0.35 \pm 0.26 (0.044–0.89) | 0.29 \pm 0.24 (8, 0.046–0.76) | 0.40 \pm 0.29 (10, 0.044–0.89) |
| PYR | 0.23 \pm 0.20 (0.09–0.86) | 0.18 \pm 0.09 (6, 0.13–0.34) | 0.28 \pm 0.25 (8, 0.09–0.86) |
| PCB 28 | 0.020 \pm 0.009 (0.006–0.037) | 0.021 \pm 0.010 (5, 0.008–0.033) | 0.020 \pm 0.009 (10, 0.006–0.037) |
| PCB 52 | 0.012 \pm 0.007 (0.003–0.024) | 0.014 \pm 0.008 (6, 0.003–0.024) | 0.011 \pm 0.005 (10, 0.003–0.023) |
| PCB101 | 0.008 \pm 0.002 (0.005–0.011) | 0.009 \pm 0.002 (4, 0.006–0.011) | 0.006 \pm 0.001 (5, 0.005–0.008) |
| α -HCH | 0.038 \pm 0.021 (0.008–0.078) | 0.056 \pm 0.013 (6, 0.039–0.076) | 0.031 \pm 0.020 (10, 0.008–0.078) |
| γ -HCH | 0.106 \pm 0.072 (0.007–0.245) | 0.136 \pm 0.078 (8, 0.030–0.245) | 0.089 \pm 0.067 (11, 0.007–0.242) |
| <i>p,p'</i> -DDE | 0.007 \pm 0.004 (0.003–0.015) | 0.008 \pm 0.003 (4, 0.006–0.012) | 0.007 \pm 0.004 (8, 0.003–0.015) |
| BDE 47 | 0.327 \pm 0.119 (0.20–0.51) | 0.265 \pm 0.046 (3, 0.228–0.317) | 0.36 \pm 0.14 (5, 0.20–0.51) |
| BDE 99 | 0.218 \pm 0.062 (0.14–0.31) | 0.195 \pm 0.024 (4, 0.161–0.214) | 0.234 \pm 0.077 (5, 0.137–0.313) |

737

738

b.

| | all samples | night-time | day-time |
|------------------|-----------------------------------|--------------------------------------|--------------------------------------|
| ACE | 0.008 \pm 0.047 (-0.026–0.10) | -0.001 \pm 0.027 (4, -0.024–0.037) | 0.019 \pm 0.072 (3, -0.026–0.10) |
| PHE | 1.24 \pm 2.10 (-0.047–7.35) | 1.19 \pm 1.96 (4, -0.047–5.55) | 1.29 \pm 2.32 (6, 0.009–7.35) |
| FLT | 0.19 \pm 0.43 (-0.46–0.95) | 0.33 \pm 0.44 (6, -0.25–0.95) | 0.073 \pm 0.40 (6, -0.46–0.73) |
| PYR | 0.081 \pm 0.21 (-0.42–0.45) | 0.18 \pm 0.17 (6, 0.038–0.45) | 0.004 \pm 0.22 (6, -0.42–0.32) |
| PCB 28 | 0.024 \pm 0.046 (-0.013–0.155) | 0.013 \pm 0.040 (7, -0.011–0.103) | 0.032 \pm 0.050 (10, -0.013–0.155) |
| PCB 52 | 0.016 \pm 0.036 (-0.011–0.120) | 0.009 \pm 0.036 (7, -0.011–0.089) | 0.020 \pm 0.038 (10, -0.004–0.120) |
| PCB101 | 0.012 \pm 0.018 (-0.005–0.044) | 0.007 \pm 0.019 (4, -0.005–0.035) | 0.018 \pm 0.018 (4, -0.001–0.044) |
| α -HCH | 0.079 \pm 0.188 (-0.048–0.675) | 0.025 \pm 0.131 (5, -0.048–0.258) | 0.107 \pm 0.212 (10, -0.019–0.675) |
| γ -HCH | 0.107 \pm 0.273 (-0.159–0.890) | 0.018 \pm 0.222 (7, -0.159–0.510) | 0.164 \pm 0.297 (11, -0.073–0.890) |
| <i>p,p'</i> -DDE | 0.001 \pm 0.005 (-0.006–0.009) | 0.002 \pm 0.004 (4, -0.001–0.007) | 0.001 \pm 0.006 (5, -0.006–0.009) |
| BDE 47 | -0.229 \pm 0.072 (-0.280–0.178) | n.d. | -0.229 \pm 0.072 (2, -0.280–0.178) |
| BDE 99 | -0.042 \pm 0.017 (-0.059–0.025) | -0.058 (1) | -0.034 \pm 0.014 (2, -0.044–0.025) |

739

740 Table 2. Concentrations in air (gaseous, ground level, $z = 1.05$ m, if >LOQ for most samples)
741 (ng m^{-3} , except PBDEs: pg m^{-3}) and surface seawater (pg L^{-1}) and fugacity ratios, f_a/f_w .

| | c_a | c_w | f_a/f_w |
|------------------|--------|-------|-----------|
| FLT | 0.35 | 18.2 | 19 |
| PYR | 0.23 | 4.4 | 59 |
| PCB 28 | 0.020 | 4.65 | 0.15 |
| PCB 52 | 0.012 | 0.54 | 0.94 |
| PCB 101 | 0.0076 | 0.84 | 0.34 |
| <i>p,p'</i> -DDE | 0.0072 | 0.84 | 0.76 |
| BDE 47 | 0.33 | 0.15 | 2600 |
| BDE 99 | 0.22 | 0.038 | 16140 |

742

743 Figure captions

744

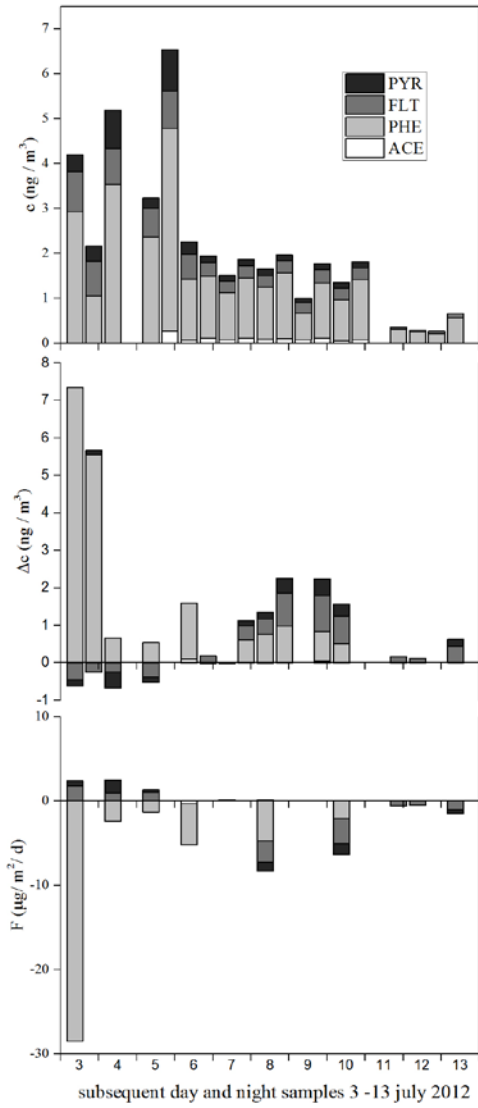
745 Fig. 1. Gaseous (a) PAH and (b) halogenated substances' concentrations at ground level, $z_1 =$
746 1.05 m (upper), vertical concentration differences, $\Delta c_z = c_{z2} - c_{z1}$, over $\Delta z = 1.75$ m (middle)
747 and vertical fluxes, $F_c = -v_{tr} \Delta c_z$ (positive = upward, negative = downward; lower). Only
748 significant data (exceeding uncertainty thresholds) shown, gaps = no data.

749

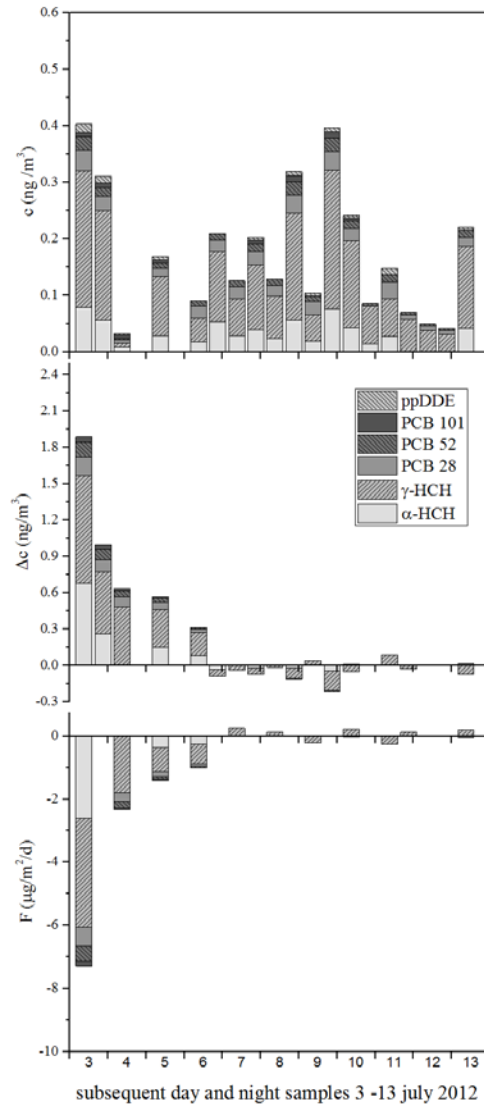
750 Fig. 2. Predicted (pink) and observed (black) concentrations (ng m⁻³) and predicted diffusive
751 air-sea exchange fluxes, F_c , (lower: red upward and blue downward, ng m⁻² d⁻¹) of selected
752 contaminants, (a) HCB, (b) PCB28, (bc) FLT and (de) BDE47 during 6-10 July 2012.

753

754 Fig. 1
 755 a.



b.

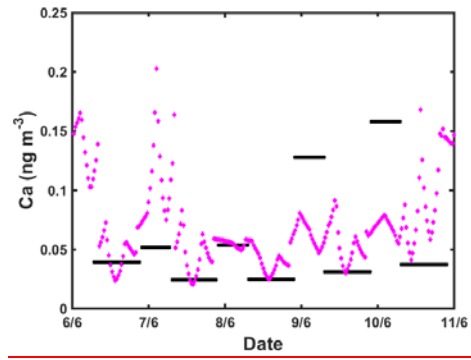


756
 757

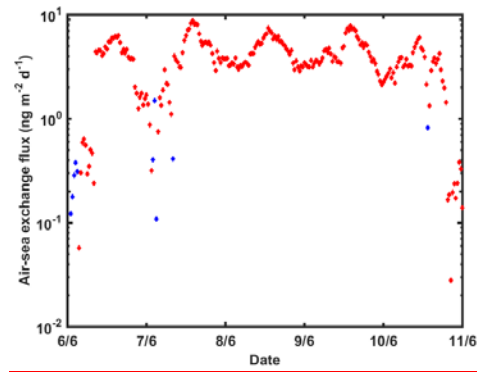
758 Fig. 2.

759

a.



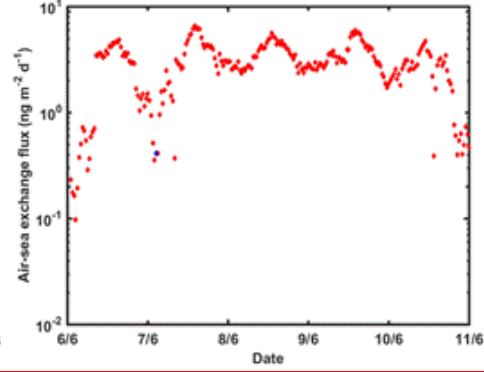
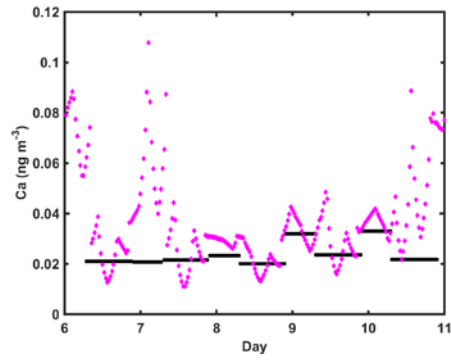
760



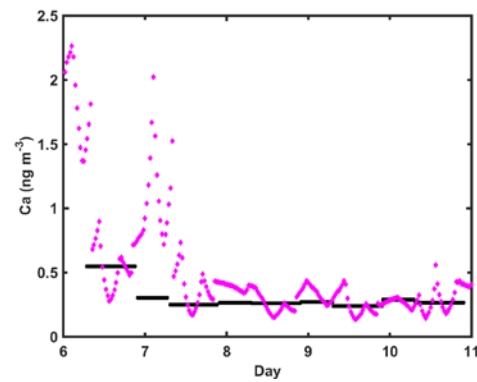
761

762

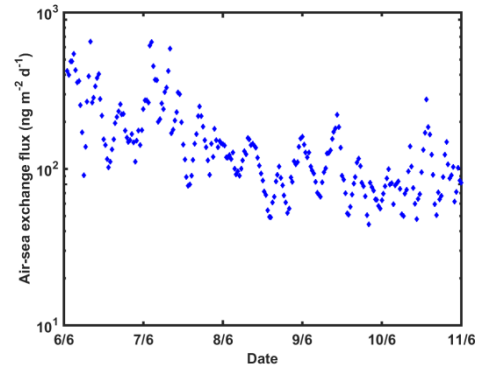
b.



c.



763



764

765

d.

